

## BROADBAND LOW NOISE OPTICAL RECEIVER UTILIZING DISTRIBUTED AMPLIFICATION

T. Bercei\*, A. Zólomy\*, G. Járó\*, A. Hilt°, T. Marozsák\*

### *Abstract*

*A new approach for the design and construction of low noise broadband optical receivers is presented utilizing distributed amplification based on hybrid integrated technology. Using extremely low noise PHEMTs as well as appropriate matching between the photodiode and the distributed amplifier result in a fairly low input equivalent noise current ( $10 \text{ pA} / \sqrt{\text{Hz}}$ ). Due to the high capacitance bypass capacitors the lower edge of the transmission band is decreased which is important for many applications.*

### **Introduction**

Wideband optical reception is a crucial problem in broadband communication networks. The present systems usually apply high speed photodiodes resistively matched to the input of monolithic transimpedance amplifiers. That approach is widely used because it provides a rather good performance at low cost. However, the noise of this approach is relatively high due to the additional noise coming from the matching resistor at the input.

Furthermore, in case of a monolithic integrated circuit the noise factor of the amplifier containing PHEMTs is usually higher than that can be achieved discrete devices. Another problem is that the capacitance of the bypass capacitors is limited by the monolithic technology. Thus the lower edge of the transmission band is at a relatively high frequency.

In this paper a new approach is presented utilizing distributed amplification based on hybrid integrated technology. Using a microstrip circuitry as well as chip capacitors and resistors a very compact amplifier construction is realized and eight octave bandwidth is achieved.

At the same time the noise performance is also improved by proper matching between the photodiode and the distributed amplifier and also by applying reactive termination for the gate line in the distributed amplifier.

The noise properties of the developed two-stage distributed amplifier can be further improved either by increasing the number of stages [1] or by choosing better transistors [2].

\* BME-MHT, Technical University of Budapest,  
H-1111 Budapest, Goldmann György tér 3, Hungary  
e-mail: t-berceli @ nov.mht.bme.hu

° TKI Rt., Innovation Company for Telecommunications  
H-1142 Budapest, Ungvár utca 64-66, Hungary

**Characterization of the pin photodiode**

To achieve the desired low noise and broad bandwidth the design of the reactive matching circuit between the photodiode and the amplifier requires a sophisticated and accurate model for the used PD94CP-S12AR1300 type pin photodiode chip [3]. This model provides a starting point for the development of the broadband optical receiver.

The top view of the photodiode chip is shown in Fig. 1.a. The chip has an active area of  $12\ \mu\text{m}$  by  $12\ \mu\text{m}$  and can work up to 50 GHz. This photodiode was tested in the frequency domain at different bias and illumination conditions both electrically and optically [4].

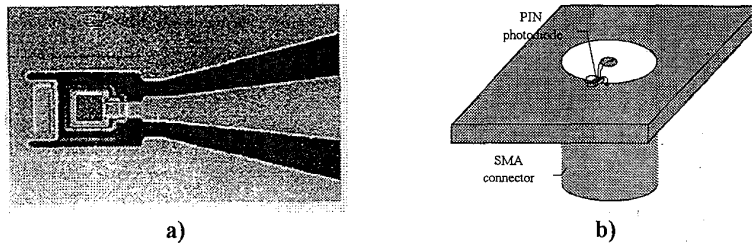


**Fig. 1** a) Top view of the used PD94CP-S12AR1300 type pin photodiode of Opto Speed. b) The diode bonded onto a SMA connector

For the measurements a HP 8510B Vector Network Analyzer extended by a HP 83420A Lightwave Component Analyzer was used. The diode was bonded onto a SMA connector as shown in Fig 1.b.

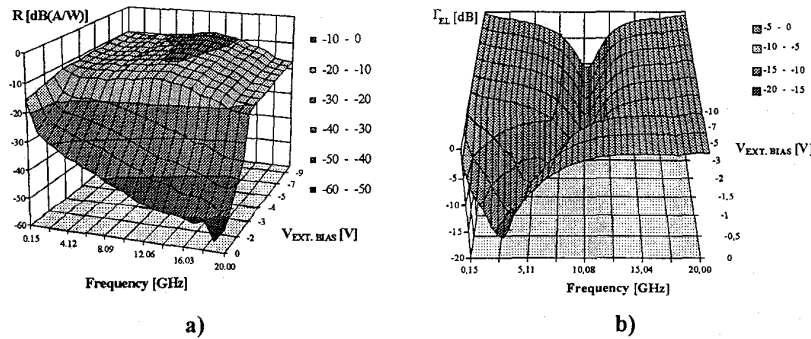


**Fig. 2.** a) Measured responsivity b) Reflection of the bonded  $12 \times 12\ \mu\text{m}^2$  Opto Speed pin photodiode chip at different modulation frequencies and external bias voltages (with  $300\ \mu\text{W}$  incident optical power)

Fig. 2.a and Fig. 2.b show the measured responsivity and electrical reflection respectively as functions of the modulation frequency and the external reverse bias voltage (which was

applied to the diode through a  $27\text{ k}\Omega$  series resistor). The frequency of the resonance in Fig 2.b is determined by the bonding inductance and the diode capacitance. The capacitance strongly depends on the bias conditions. Fig. 3.a shows the variance of the capacitance versus the bias with and without illumination. The results emphasize the importance of the strong reverse bias voltage applied to the photodiode in order to avoid sudden changes in the diode properties and to achieve large bandwidth. The equivalent circuit shown in Fig. 3.b was extracted from the measured electrical reflection data by optimization.

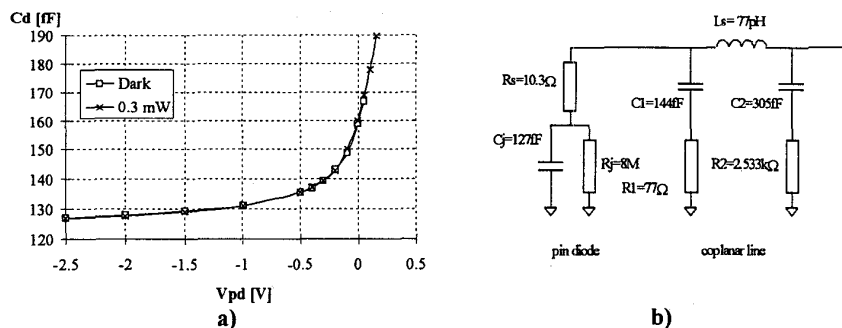


Fig. 3 a) Variation of the photodiode capacitance b) Equivalent circuit of the photodiode

#### Design of the two-stage hybrid integrated distributed amplifier

As a starting point a two-stage low noise distributed amplifier was designed between  $50\ \Omega$  terminations. The optical receiver was constructed using this amplifier by optimizing the circuit with reactive termination at the input.

For the design of the amplifier the HP-ATF35376 type PHEMT was chosen as an active device due to its low noise, low values of parasitics and input and output capacitances [2]. The transistor model is shown in Fig. 4.

#### Gain-bandwidth considerations

The ideal, lumped element, loss free case when the transistors of the amplifier consist of an input and output capacitance and a transconductance is shown in Fig. 5.

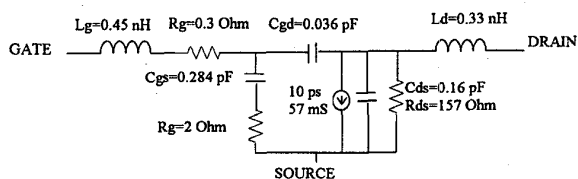


Fig. 4 Equivalent circuit of the applied ATF35376 PHEMT from HP

The input capacitor of the transistor is usually higher than the output one. So the bandwidth is limited by the cut off frequency of the input artificial transmission line if the amplifier is working between the same terminating impedances.

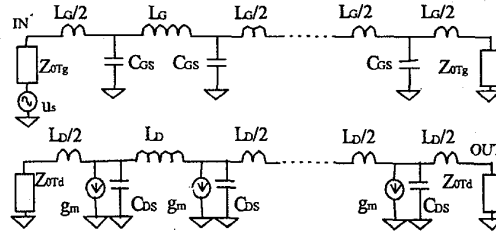


Fig. 5 N-stage loss free distributed amplifier

Using the capacitance values given in Fig. 4 the cut off of the input line in a 50 Ω system is  $\omega_c = 2/\sqrt{L_G C_{GS}} = 22 \text{ GHz}$  [5]. The value of  $\omega_c$  is independent of the number of stages. The available power gain for the ideal lossless case is given by Eq. 1 [1]:

$$G = \frac{N^2 g_m^2 Z_{0g} Z_{0d}}{4} \quad (1)$$

where N is the number of sections and  $Z_{0g}$  and  $Z_{0d}$  are the characteristic impedances of the gate and drain lines, respectively. In our transistor model the transconductance is  $g_m = 57 \text{ mS}$ . When the losses are neglected, this amplifier produces a gain of 9 dB in two-stages between 50 Ω terminations.

The parasitics and the losses degrade the performance significantly. The bandwidth is limited mainly by the effect of the series parasitic inductances ( $L_{GP}$ ,  $L_{DP}$ ). Again the cut off frequency is determined by the input line due to its higher elements values. According to this and for the simplicity we have calculated the voltage gain of an amplifier having identical input and output lines ( $C_{GS} = C_{DS} = C$ ,  $L_{GP} = L_{DP} = L_B$ ,  $L_G = L_D = L$ ). The amplifier schematic is given in Fig. 6.

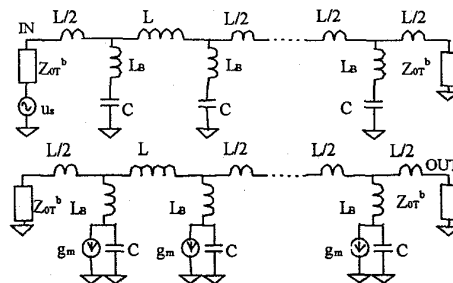


Fig. 6. Distributed amplifier structure with parasitic inductances

The voltage gain in this case is given by Eq. 2 [6].

$$A_v(\omega) = \frac{1}{2} \sqrt{\frac{L}{C}} \frac{Ng_m}{(1 - \omega^2/\omega_{c2}^2) \sqrt{1 - \omega^2/\omega_{c1}^2}} e^{-jN\theta_b} \quad (2)$$

where

$$\theta_b = 2 \arctg \left( \frac{\omega \sqrt{LC}}{2 \sqrt{1 - (\omega/\omega_{c1})^2}} \right), \quad \omega_{c1} = \frac{2}{\sqrt{C(4L_B + L)}}, \quad \omega_{c2} = \frac{1}{\sqrt{C L_B}}, \quad L = Z_0^2 C. \quad (3)$$

According to this results the bandwidth is limited by the first cut-off frequency ( $\omega_{c1}$ ) which is significantly lower than in the ideal case due to the very strong effect of the series parasitic inductance  $L_B$ . Substituting the element values of the equivalent circuit ( $C=0.284$  pF,  $L_B=0.45$  nH) and the value of the characteristic impedance ( $Z_0=50 \Omega$ ) the calculated cut-off frequency of the amplifier is  $f_c = \omega_{c1}/2\pi = 11.95$  GHz. This result also does not depend on the number of stages.

The gain is limited by the losses. Most of the losses is caused by the transistor parasitics ( $R_G$ ,  $R_{DS}$ ). The power gain for the lossy case is given by Eq. 4 [5] if transmission lines are used between the stages:

$$G = \frac{g_m^2 Z_{0g} Z_{0d}}{4} \left| \frac{\exp(-N\alpha_g l_g) - \exp(-N\alpha_d l_d)}{\alpha_g l_g - \alpha_d l_d} \right|^2 \quad (4)$$

where  $\alpha_g$  and  $\alpha_d$  are the attenuation factors of the gain and drain lines, respectively. Using the above mentioned transistor elements the gain of a two-stage amplifier operating between  $50 \Omega$  terminations ( $Z_{0g} = Z_{0d} = 50 \Omega$ ) is approximately 7 dB. In a real amplifier the gain may differ from this value because of the reflections in the gate and drain lines. The difference is 1-2 dB with a simultaneous gain ripple.

#### Simulation of the amplifier

According to the results of the previous subsection a gain of 8 dB was chosen as a goal in the 1–10 GHz band during the optimization. The basic structure for the simulation is shown in Fig. 6 [7] comprising the PHEMT model given in Fig. 4. Due to the large dimensions of the transistor case relatively long drain and gate lines needed between the consecutive stages. This requirement can be fulfilled by using a low dielectric constant substrate material like the Duroid 5880 which has an  $\epsilon_r = 2.2$ . The microstrip discontinuities and the additional elements were put into the circuit step by step during the simulation.

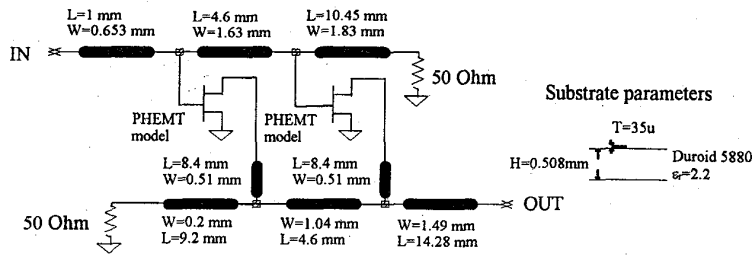


Fig. 6. Basic amplifier structure for the simulation

Tapered lines were introduced for replacing the sudden changes in the characteristic impedance of the microstrip line caused by its width disturbances. The final layout of the amplifier is shown in Fig. 7.

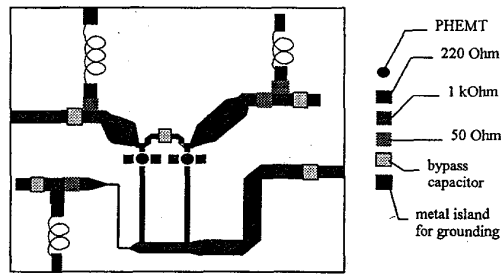


Fig. 7. Layout of the realized hybrid amplifier

The measured gain and noise figure are presented in Fig. 8. The gain has a value of  $7 \pm 1$  dB. The noise figure is better than 5.2 dB and has a minimum value of 2.2 dB at 8.5 GHz. The shape of the curve is close to the theoretical one given by [2]. Numerical calculations have shown that the main contribution to the noise comes from the gate termination and from the first transistor.

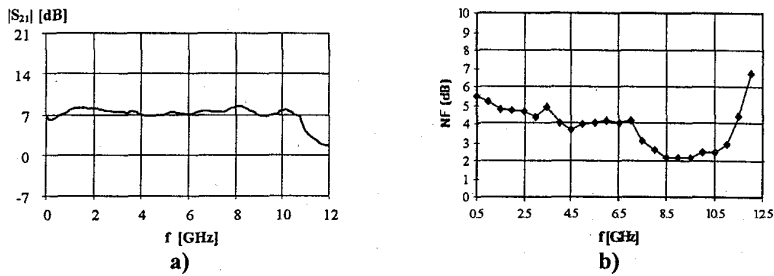


Fig. 8 a) The measured gain b) Noise figure of the realized amplifier

**Design of the hybrid integrated optical receiver**

The design of an optical receiver comprising a pin photodiode and a distributed amplifier has a task to match a capacitive current generator (pin diode) to an amplifier with 50 Ω input impedance over a wide frequency range with a simultaneous low noise level.

The characteristics of an optical receiver are not only determined by the parameters of the photodiode and the distributed amplifier, but they are also greatly influenced by the matching circuit between them [8,9]. The gain and the input equivalent noise current of the amplifier are compared in different matching configurations.

A two-stage distributed amplifier matched to 50 Ω impedance is modeled with lumped elements. Fig. 9 shows the schematic of the amplifier.

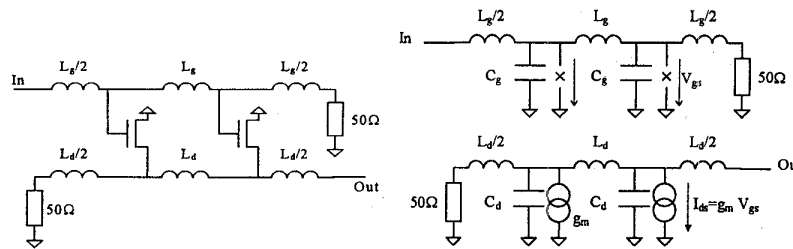


**Fig. 9** Schematic of a two-stage distributed amplifier with lumped elements

Inserting the transistor model (represented by the gate and drain capacitances, and voltage controlled current source) into the amplifier leads to an LC artificial transmission line structure. For calculating the input noise current density, the noise sources in the distributed amplifier were modeled. The thermal noise generated by the resistors was modeled by a parallel noise current source. The noise equivalent circuit of the transistors comprises two correlated noise sources as shown in Fig 10.

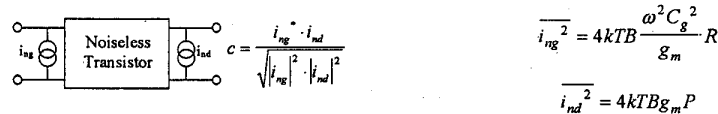


**Fig. 10** Noise model of the transistor

The currents of these gate and drain noise sources were calculated using the equations of Van der Ziel et al. where the parameters R and P are varying with the drain current. It can be shown that the correlation coefficient can be written as:  $c = c_r + i c_i = 0 + 0.35i$ . For our PHEMT values, the gain of the amplifier is 8 dB, while the input and the output reflections ( $|S_{11}|$  and  $|S_{22}|$ ) are smaller than -20 dB in the frequency range of 0-20 GHz. Taking  $C_g = 0.2$  pF,

$C_d = 0.1 \text{ pF}$  and  $g_m = 50 \text{ mS}$ , the value of  $L_g$  and  $L_d$  are  $530 \text{ pH}$  and  $235 \text{ pH}$ , respectively. Fig. 11 shows the equivalent circuit and noise model (in this case up to  $20 \text{ GHz}$ ) of the distributed amplifier of Fig. 9.

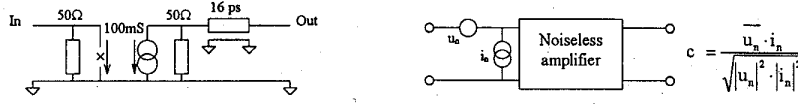


Fig. 11 Equivalent circuit and noise model of the distributed amplifier

This general simplified distributed amplifier model consists of an ideal amplifier and a delay line. The noise of the amplifier is substituted with a correlated voltage and current noise source pair. These models were used to compare the different photodiode and amplifier interconnections. For the comparison of the O/E conversions of the optical receivers the transimpedance was calculated. Usually the noise properties of optical receivers are described by the equivalent input noise current. In Fig. 12 four different matching techniques are presented.

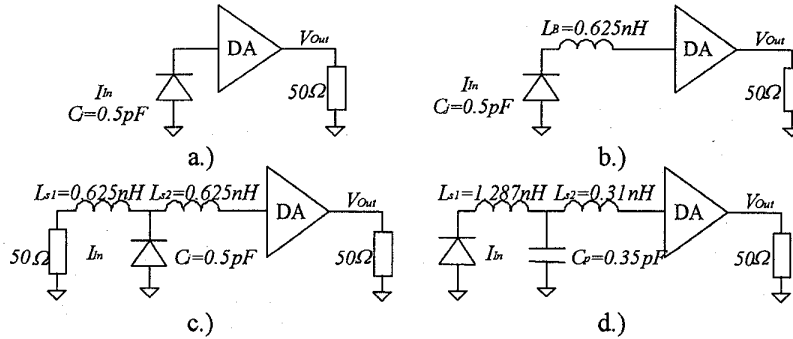


Fig. 12 Different matching circuit configurations

The noise and the bandwidth were compared for all matching methods using the latter models. The photodiode is modeled with a parallel capacitor and a current generator representing the O/E conversion. The circuit parameters are chosen for maximally flat gain (except the resistive matching where the interconnecting circuit elements are chosen for maximally flat input impedance). Fig. 13 shows the calculated transfer impedance and equivalent input noise current densities of the analyzed circuits. The optical receiver applying resistive matching has  $6 \text{ dB}$  less amplification and greater noise than the others

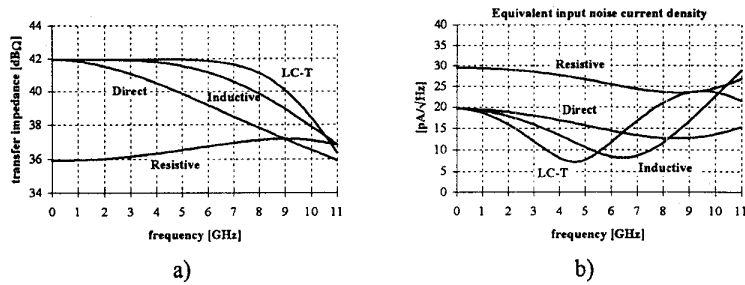


Fig. 13. a) The transimpedance vs. frequency b) Equivalent noise current vs. frequency for the four matching methods

Comparing the analyzed circuits, the best solution is the non-resistive LC T-section considering both the gain and noise performance. However due to the low photodiode capacitance the realization of the LC-T type matching circuit is difficult.

### Optical receiver

Due to the realization difficulties the LC-T type matching is unattractive. The performance of the matching circuit comprising only a series bonding inductance is almost as good as the performance of the best solution (see Fig. 13) but due to the very simple construction of this method the realization problems are eliminated. The picture of the hybrid integrated optical receiver using inductive matching is presented in Fig. 14.

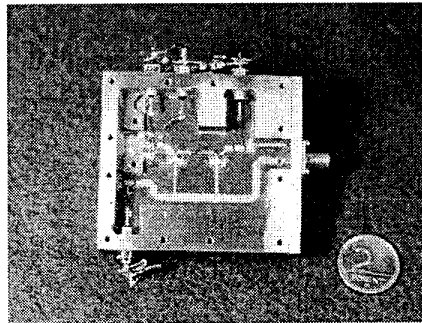


Fig. 14 Picture of the photoreceiver

Fig. 15 shows the measured responsivity. The frequency response can be further improved either by tuning or by the more accurate realization of the bonding inductance value between the diode and the amplifier.

### Measurement of the equivalent input noise current density

The noise measurement method is shown in Fig. 16. Due to the low output noise power of the receiver a very high gain amplifier is used to be able to detect it by a conventional spectrum analyzer (HP 8394). As a calibration a  $50\ \Omega$  termination is connected to the input of the high gain amplifier.

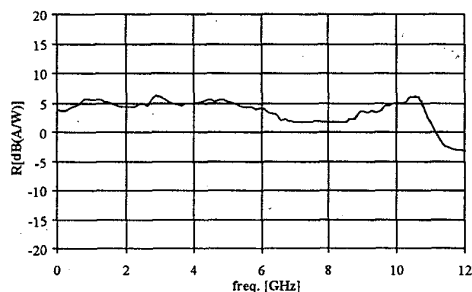


Fig. 15 Measured responsivity of the photoreceiver

The measured noise power of this case at the input of the spectrum analyzer is used in Eq. (5) to calculate the density of the noise voltage at the output of the optical receiver. From this data the equivalent input noise current density can be calculated by Eq. (6) using the value of the transimpedance of the two-stage distributed amplifier.

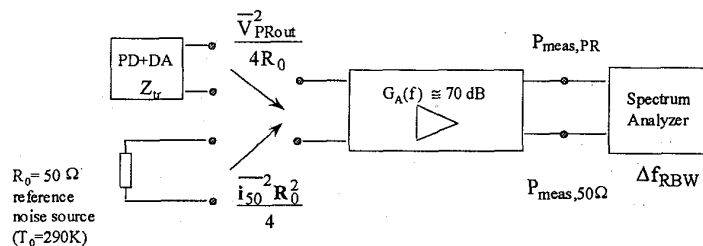


Fig. 16 Noise measurement setup

For the calculation a receiver output impedance of  $50\ \Omega$  is assumed.

$$\overline{V}_{PRout}^2(f) = \frac{4R_0 (P_{meas,PR} - P_{meas,50\Omega})}{\Delta f_{RBW} G_A(f)} + i_{50}^{-2} R_0^2 \quad (5)$$

$$i_{eqPRin}^{-2}(f) = \frac{\overline{V}_{PRout}^2}{Z_{tr}^2} [\text{pA}/\sqrt{\text{Hz}}] \quad (6)$$

The measured input noise current density is shown in Fig. 17.

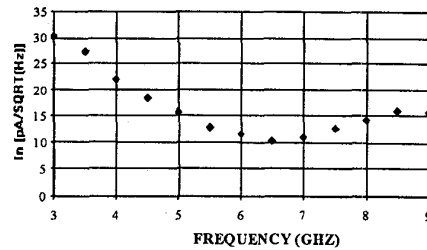


Fig. 17 Measured input noise current density

### Conclusions

A hybrid integrated optical receiver utilizing a two-stage distributed amplifier was presented. The applied pin photodiode has been investigated at different conditions and an accurate equivalent model was developed. A low noise distributed amplifier was designed using commercially available encapsulated PHEMTs. The matching between the photodiode and amplifier has been investigated and a proper matching circuit has been chosen. The optical receiver has a bandwidth of 8 octave from 40 MHz and low input equivalent noise.

### Acknowledgment

We thank OptoSpeed Switzerland for generously offering the high speed photodiodes. The authors also wish to thank to Prof. C.S. Aitchison for the important discussions. The work was supported by the Copernicus Program and the FRANS project of the European Union and the Hungarian Scientific Research Fund 'OTKA' (Project No. T017295, F024113, T019839, T019857).

### References

- [1] Colin S. Aitchison: "The Intrinsic Noise Figure of the MESFET Distributed Amplifier", IEEE Trans. on Microwave Theory and Techniques, vol. 33, pp. 460-466, June 1985.
- [2] Hewlett Packard: "GaAs & Silicon Product Designers Catalog" 1994.
- [3] Opto Speed: "PD94CP-S12AR1300 InGaAs pin photodiode chip data sheets", Opto Speed S.A., Via Cantonale, Mezzovico, CH - 6805 Switzerland, 1995.
- [4] A. Hilt, G. Járó, A. Zólomy, B. Cabon, T. Bercei, T. Marozsák: "Microwave Characterization of High-Speed pin Photodiodes", proc. of COMITE'97, 9<sup>th</sup> Conference on Microwave Techniques, pp. 21-24, Pardubice, Czech Republic, October 1997.
- [5] Thomas T. Y. Wong: "Fundamentals of Distributed Amplification", Artech House, Boston 1993.

- [6] A. Zólomy , A. Hilt, A. Baranyi, G. Járó: "Microwave Distributed Amplifier in Hybrid Integrated Technology", proc. of the 13<sup>th</sup> European Conference on Circuit Theory and Design, ECCTD'97, Vol.3, pp. 1374-1377, Budapest, Hungary, September 1997.
- [7] A. Zólomy, G. Járó, A. Hilt, A. Baranyi, J. Ladvánszky: "Wideband Distributed Amplifier Using Encapsulated HEMTs", Advanced NATO Research Workshop, Sozopol, Bulgaria, September 1996. Horst Groll and Ivan Nedkov ed. : "Microwave Physics and Techniques", NATO ASI Series, 3-Vol.33, pp. 315-320, Kluwer Academic Publishers, Dordrecht, Boston, London, ISBN 0-7923-4582-7.
- [8] G. Járó, A. Hilt, A. Zólomy, T. Berceli: "Noise Properties of Optical Receivers Using Distributed Amplification", Journal on Communications, Vol. XLVIII, pp. 31-34, August, 1997.
- [9] T. Berceli, A. Zólomy, G. Járó, A. Hilt, T. Marozsák: "Low Noise Optical Receiver With Multi-Octave Bandwidth", submitted for publication to Optical and Quantum Electronics